Forward-backward asymmetry in the $H \to Z\gamma \to \bar{f}f\gamma$ decay

A. I. Hernández-Juárez,* D. Watko, A. Fernández-Téllez, and G. Tavares-Velasco
Facultad de Ciencias Físico Matemáticas, Benemérita Universidad Autónoma de Puebla, Apartado Postal 1152, Puebla, Puebla, México

(Received 6 May 2026; accepted 17 August 2026; published 21 September 2026)

We study the forward-backward asymmetry in the three-body decay process $H \to Z\gamma \to \bar{f}f\gamma$, induced by complex form factors in the $HZ\gamma$ vertex. To estimate its magnitude, we derive constraints on the real and imaginary parts of the CP-violating form factor $h_3^{Z\gamma}$ using current LHC measurements, obtaining upper limits of about 0.9 GeV. These bounds are of the same order of magnitude as those derived from electric dipole moments. We find that the asymmetry can reach values of order 10^{-1} and may be accessible at the HL-LHC.

DOI: 10.1103/7ctd-6fmw

I. INTRODUCTION

The $H \to Z\gamma$ decay attracted considerable attention following the first experimental evidence reported by the ATLAS and CMS collaborations, with a measured signal strength of $\mu^{Z\gamma} = 2.2 \pm 0.7$ [1,2]. Although this result was consistent with the Standard Model (SM) within 1.9σ, it was regarded as a potential window into new physics. In particular, the central value suggested a possible enhancement with respect to the SM prediction, motivating further theoretical and phenomenological studies. Several works explored possible explanations for this deviation within extensions of the SM, including two-Higgs-doublet models [3–5], nonsupersymmetric scenarios [6], the minimal supersymmetric SM [7,8], and models with additional fermions or gauge bosons [9–14]. In this context, CP violation in the $HZ\gamma$ vertex was also proposed to explain the deviations in $\mu^{Z\gamma}$ reported by the LHC [15]. These contributions arise from flavor-changing neutral currents (FCNC) involving the Z and Higgs boson.

The CP-even and CP-odd form factors can be introduced in the most general $HZ\gamma$ effective vertex as follows:

$$\Gamma^{\mu\nu}_{Z\gamma H} = h_1^{Z\gamma}\left\{g^{\mu\nu} + \frac{2}{m_Z^2 - m_H^2} p_1^\nu p_2^\mu\right\} + \frac{1}{m_Z^2} h_3^{Z\gamma} \epsilon^{\mu\nu\alpha\beta} p_{1\alpha} p_{2\beta}, \tag{1}$$

where we adopt the kinematics shown in Fig. 1. The form factors $h_1^{Z\gamma}$ and $h_3^{Z\gamma}$ are CP conserving and CP violating, respectively. The notation in Eq. (1) implies that the form factors have units of mass. Furthermore, gauge invariance relates $h_1^{Z\gamma}$ to $h_2^{Z\gamma}$, and therefore the latter is not considered. In the SM, only $h_1^{Z\gamma}$ is generated at the one-loop level [16–19], with dominant contributions arising from W boson loops. Fermion loops also contribute, giving rise to a small imaginary part. The total electroweak contribution is given by

$$h_1^{Z\gamma} = (-3.22 \times 10^{-1} + i2.6 \times 10^{-4})\ \text{GeV}. \tag{2}$$

QCD corrections have been computed and are known to be small [20–22], whereas next-to-leading-order electroweak corrections can reach ∼7% of the leading contribution [4]. Imaginary parts such as that in Eq. (2) also arise in other SM radiative corrections [23–25] and can play an important role in CP-violating observables [26–28]. The study of CP-odd effects in the $HZ\gamma$ coupling has been performed in γp [29] and e^+e^- colliders [30,31], as well as through polarized observables [32–34]. Further studies can be found in Refs. [35–37].

The general conditions for generating CP-violating observables in the $HZ\gamma$ coupling with three reconstructable final-state particles were discussed in Ref. [39]. In this framework, such observables arise from the interference between weak phases in the Higgs Lagrangian and strong phases induced by the Breit-Wigner widths of different intermediate particles. Similar interference mechanisms have been studied in B-meson physics [40–42], top-quark decays [40,43], and supersymmetric models [44].

In the particular case of the $HZ\gamma$ coupling, CP-violating effects can be probed through a forward-backward asymmetry ($\mathcal{A}_{FB}$). Such an asymmetry can arise either from the interference between CP-even and CP-odd complex form factors in the $HZ\gamma$ vertex [45–47], or from the interference

*Contact author: alan.hernandezjua@alumno.buap.mx

Published by the American Physical Society under the terms of the Creative Commons Attribution 4.0 International license. Further distribution of this work must maintain attribution to the author(s) and the published article's title, journal citation, and DOI. Funded by SCOAP³.

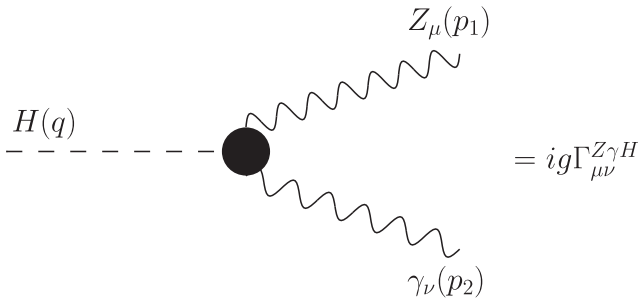


FIG. 1. The $HZ\gamma$ vertex function. The Feynman diagrams in this work are created with JaxoDraw [38].

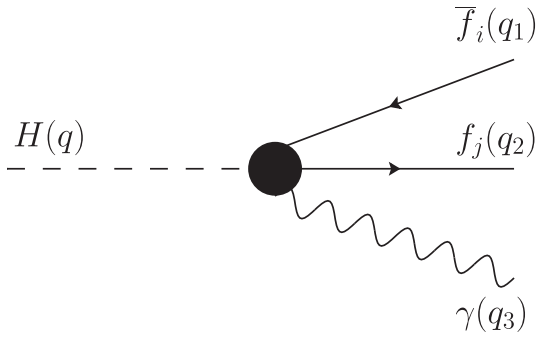


FIG. 2. Kinematic configuration and momentum assignments for the $HZ\gamma$ vertex.

of the signal with intermediate states or background processes [48], such as $H \to \gamma^*\gamma \to \overline{\ell}\ell\gamma$ [39], $H \to ZZ \to 4\ell$ [49], $gg \to ZZ \to 4\ell$ [50], $gg \to \gamma^*\gamma \to \overline{\ell}\ell\gamma$ [51], and $gg \to Z\gamma \to \overline{\ell}\ell\gamma$ [52]. However, the former mechanism, which originates solely from the $HZ\gamma$ vertex, has received comparatively less attention in recent studies [53].

In this work, we focus on the forward-backward asymmetry induced by complex CP-conserving and CP-violating form factors in the $HZ\gamma$ vertex. We show that this asymmetry can be generated without the need for interference with background processes. Furthermore, bounds on the CP-violating form factor $h_3^{Z\gamma}$ are obtained from current LHC data and used to evaluate the size of the forward-backward asymmetry. The manuscript is organized as follows: in Sec II, we compute the $H \to Z\gamma \to \bar{f}f\gamma$ decay amplitude and derive the forward-backward asymmetry. In Sec. III, limits on the CP-violating form factor $h_3^{Z\gamma}$ are obtained, whereas in Sec. IV we present a numerical analysis of the CP-violating effects and the possibility of observing $\mathcal{A}_{FB}$ in the high-luminosity LHC (HL-LHC). Finally, in Sec. V, we present our conclusions.

II. *CP* VIOLATION IN THE $H \to Z\gamma \to \bar{f}f\gamma$ DECAY

In this section, we analyze the effects of the CP-violating form factor $h_3^{Z\gamma}$ on the decay $H \to Z\gamma \to \bar{f}f\gamma$. Since the form factor $h_1^{Z\gamma}$ is complex within the SM, we allow $h_3^{Z\gamma}$ to be complex as well. To identify the role of the absorptive parts, it is convenient to write $h_i^{Z\gamma}$ $(i = 1, 3)$ as

$$h_i^{Z\gamma} = \mathrm{Re}[h_i^{Z\gamma}] + i\,\mathrm{Im}[h_i^{Z\gamma}], \quad i = 1, 3. \tag{3}$$

In the SM, complex CP-conserving form factors have been studied in scenarios where at least one of the particles in the vertex is off-shell [23–25]. In contrast, CP-violating anomalous couplings with nonzero imaginary parts can appear in extensions of the SM, such as in ZZV^* and $Z\gamma V^*$ $(V = Z, \gamma)$ vertices [54,55], as well as in quark-gluon interactions [56–58].

We follow the momentum assignment shown in Fig. 2 and perform the calculations with FeynCalc [59–62]. The process $H \to Z\gamma \to \bar{f}f\gamma$ proceeds through an intermediate Z boson decaying into a fermion pair. The corresponding amplitude can thus be written as the product of the $H \to Z\gamma$ and $Z \to \bar{f}f$ amplitudes, linked by the Z-boson propagator:

$$\begin{aligned}\mathcal{M}(H \to Z\gamma \to \bar{f}f\gamma) &= -i\frac{g}{k^2 - m_Z^2 + i\Gamma_Z m_Z}\mathcal{M}^{\mu\nu}(H \to Z(k)\gamma) \\ &\quad \times \mathcal{M}_\mu(Z(k) \to \bar{f}f)\epsilon_\nu^*(p_3, \lambda).\end{aligned} \tag{4}$$

Since the fermions are treated as massless, the term $k^\sigma k^\mu/m_Z^2$ in the Z boson propagator does not contribute to the squared amplitude and can therefore be safely neglected. Using Eq. (1), the $H \to Z\gamma$ decay amplitude, including complex form factors, can be written as

$$\begin{aligned}\mathcal{M}^{\mu\nu}(H \to Z(k)\gamma) &= ig\left[(\mathrm{Re}[h_1^{Z\gamma}] + i\,\mathrm{Im}[h_1^{Z\gamma}])\left\{g^{\mu\nu} + \frac{2}{m_Z^2 - m_H^2}k^\nu q_3^\mu\right\}\right. \\ &\quad \left. + \frac{1}{m_Z^2}(\mathrm{Re}[h_3^{Z\gamma}] + i\,\mathrm{Im}[h_3^{Z\gamma}])\epsilon^{\mu\nu\alpha\beta}k_\alpha q_{3\beta}\right],\end{aligned} \tag{5}$$

with $k = q_1 + q_2$. For the Z boson decay to fermions, the amplitude is

$$\mathcal{M}^\mu(Z(k) \to \bar{f}f) = i\frac{g}{c_W}\bar{u}(q_1)\gamma^\mu(g_V - \gamma_5 g_A)u(q_2). \tag{6}$$

Following the phase-space parametrization detailed in Appendix A 4, the differential partial width can be expressed as

$$\frac{d\Gamma}{dK\,d\cos\theta} = \frac{m_H^2 - m_Z^2}{512\pi^3 m_H^3}\mathcal{M}^2(H \to Z\gamma \to \bar{f}f\gamma), \tag{7}$$

where $K \equiv k^2$ denotes the invariant mass of the Z boson. The angle θ is defined between the antifermion three-momentum $\vec{q}_1$ and the x axis in the Z rest frame, as shown in Fig. 6. The corresponding squared amplitude is given by

$$\mathcal{M}^2 = \frac{4g^4 N_c}{c_W^2 m_Z^2((k^2-m_Z^2)^2+m_Z^2\Gamma_Z^2)}\Big[(g_A^2+g_V^2)|h_3^{Z\gamma}|^2(q_1\cdot q_3)^2 - 4(q_1\cdot q_3)\Big(g_A g_V \,\mathrm{Im}\,[h_1^{Z\gamma}(h_3^{Z\gamma})^*]m_Z^2 + 2(g_A^2+g_V^2)|h_1^{Z\gamma}|^2\frac{m_Z^4(q_2\cdot q_3)}{(m_H^2-m_Z^2)^2}\Big) + (g_A^2+g_V^2)|h_1^{Z\gamma}|^2 m_Z^4 + 4g_A g_V \,\mathrm{Im}\,[h_1^{Z\gamma}(h_3^{Z\gamma})^*]m_Z^2(q_2\cdot q_3) + (g_A^2+g_V^2)|h_3^{Z\gamma}|^2(q_2\cdot q_3)^2.\Big], \tag{8}$$

where N_c corresponds to the number of colors ($N_c = 1$ for leptons). The squared amplitude depends on the quadratic terms $|h_i^{Z\gamma}|^2$ and the interference term $\mathrm{Im}\,[h_1^{Z\gamma}(h_3^{Z\gamma})^*]$, which are defined as

$$|h_i^{Z\gamma}|^2 = \mathrm{Re}[h_i^{Z\gamma}]^2 + \mathrm{Im}[h_i^{Z\gamma}]^2, \tag{9}$$

$$\mathrm{Im}\,[h_1^{Z\gamma}(h_3^{Z\gamma})^*] = \mathrm{Im}[h_1^{Z\gamma}]\mathrm{Re}[h_3^{Z\gamma}] - \mathrm{Re}[h_1^{Z\gamma}]\,\mathrm{Im}[h_3^{Z\gamma}]. \tag{10}$$

Additionally, the $\mathcal{M}^2$ is expressed in terms of the Lorentz invariants $q_i\cdot q_3$ ($i = 1, 2$), whose explicit forms in the Higgs rest frame are given in Appendix A 3. Since the Z boson produced in the decay is on-shell, we employ the narrow-width approximation:

$$\lim_{m_Z\Gamma_Z\to 0}\frac{1}{(k^2-m_Z^2)^2+m_Z^2\Gamma_Z^2} = \delta(k^2-m_Z^2)\frac{\pi}{m_Z\Gamma_Z}, \tag{11}$$

which allows the analytic integration over the invariant mass $K = k^2$. The differential partial width can be expressed as follows:

$$\frac{d\Gamma(H\to Z\gamma\to \bar{f}f\gamma)}{d\cos\theta} = \frac{g^4(m_H^2-m_Z^2)N_c}{1024c_W^2 m_H^3 m_Z^3\pi^2\Gamma_Z}[-16g_A g_V \,\mathrm{Im}\,[h_1^{Z\gamma}(h_3^{Z\gamma})^*] \times m_Z^2(m_H^2-m_Z^2)\cos\theta + (g_A^2+g_V^2)\{4|h_1^{Z\gamma}|^2 m_Z^4 + |h_3^{Z\gamma}|^2(m_H^2-m_Z^2)^2\} \times (1+\cos^2\theta)]. \tag{12}$$

The term proportional to interference $\mathrm{Im}\,[h_1^{Z\gamma}(h_3^{Z\gamma})^*]$ is odd under $\cos\theta\to-\cos\theta$ and therefore generates a forward-backward asymmetry in the angular distribution, which provides a signal of CP violation. The structure of the differential partial width in Eq. (12) is similar to that found in Ref. [39]. In that case, the corresponding width is generated by the interference between the $H\to\gamma^*\gamma$ and $H\to Z\gamma$ intermediate processes, which contribute to the same three-body final state.

Integrating Eq. (12) yields

$$\Gamma(H\to Z\gamma\to\bar{f}f\gamma) = \frac{g^4(g_A^2+g_V^2)(m_H^2-m_Z^2)N_c}{384c_W^2 m_H^3 m_Z^3\pi^2\Gamma_Z} \times [4|h_1^{Z\gamma}|^2 m_Z^4 + |h_3^{Z\gamma}|^2(m_H^2-m_Z^2)^2], \tag{13}$$

which can be expressed in terms of the partial width and branching ratio of the $H\to Z\gamma$ and $Z\to\bar{f}f$ decays, respectively. These quantities are given by

$$\Gamma(H\to Z\gamma) = g^2\frac{m_H^2-m_Z^2}{32\pi m_H^3 m_Z^4}\{4|h_1^{Z\gamma}|^2 m_Z^4 + |h_3^{Z\gamma}|^2(m_H^2-m_Z^2)^2\} \tag{14}$$

$$\mathcal{B}(Z\to\bar{f}f) = \frac{g^2 m_Z N_c}{12\pi c_W^2\Gamma_Z}(g_A^2+g_V^2). \tag{15}$$

The partial width in Eq. (13) depends quadratically on $h_3^{Z\gamma}$, whereas the angular distribution in Eq. (12) includes linear terms. As a result, angular observables exhibit enhanced sensitivity to the CP-odd form factor. We therefore concentrate on the forward-backward asymmetry.

A. Forward-backward asymmetry

The CP-violating effects in the $HZ\gamma$ vertex can be probed through the forward-backward asymmetry ($\mathcal{A}_{FB}$) in the angular distribution of the final-state fermions. This asymmetry may arise from interference between the signal and background processes [39,50–52]. However, as indicated by Eq. (12), a nonvanishing $\mathcal{A}_{FB}$ can also be generated directly from the decay $H\to Z\gamma\to\bar{f}f\gamma$, even in the absence of background contributions. The forward-backward asymmetry is defined as

$$\mathcal{A}_{FB} = \frac{\int_0^1 d\cos\theta\frac{d\Gamma(H\to Z\gamma\to\bar{f}f\gamma)}{d\cos\theta} - \int_{-1}^0 d\cos\theta\frac{d\Gamma(H\to Z\gamma\to\bar{f}f\gamma)}{d\cos\theta}}{\int_0^1 d\cos\theta\frac{d\Gamma(H\to Z\gamma\to\bar{f}f\gamma)}{d\cos\theta} + \int_{-1}^0 d\cos\theta\frac{d\Gamma(H\to Z\gamma\to\bar{f}f\gamma)}{d\cos\theta}}. \tag{16}$$

Although this asymmetry has been discussed in the literature [45–47], to the best of our knowledge, it has

not been presented explicitly in analytic form. After performing the angular integration in Eq. (16), we obtain

$$\mathcal{A}_{FB} = \frac{6 g_A g_V m_Z^2 (m_H^2 - m_Z^2) N_c}{(g_A^2 + g_V^2)} \times \left\{ \frac{-\,\mathrm{Im}\,[h_1^{Z\gamma} (h_3^{Z\gamma})^*]}{4|h_1^{Z\gamma}|^2 m_Z^4 + |h_3^{Z\gamma}|^2 (m_H^2 - m_Z^2)^2} \right\}. \quad (17)$$

From this expression, it follows that a nonvanishing $\mathcal{A}_{FB}$ requires CP-violating and complex form factors. Since $h_1^{Z\gamma}$ is complex in the SM, a nonzero $h_3^{Z\gamma}$ is sufficient to induce the forward-backward asymmetry. The magnitude of $\mathcal{A}_{FB}$ is controlled by the real and absorptive parts of $h_3^{Z\gamma}$. Consequently, estimating the size of the asymmetry requires an exploration of the allowed parameter space of the CP-violating form factor.

III. BOUNDS ON $h_3^{Z\gamma}$

In this section, we obtain constraints on the real and imaginary parts of the CP-violating form factor $h_3^{Z\gamma}$ to evaluate the $\mathcal{A}_{FB}$ asymmetry. In Ref. [15], it was shown that, in the absence of new-physics effects in Higgs production, the signal strength of the $gg \to H \to Z\gamma$ decay can be approximated as

$$\mu^{Z\gamma} \approx \frac{\mathcal{B}^{\mathrm{SM}}(H \to Z\gamma) + \delta\Gamma^{CP}(H \to Z\gamma)/\Gamma_H}{\mathcal{B}^{\mathrm{SM}}(H \to Z\gamma)} \quad (18)$$

where $\mathcal{B}^{\mathrm{SM}}(H \to Z\gamma)$ and Γ_H denote the SM branching ratio for the $H \to Z\gamma$ decay and the total width of the Higgs boson, respectively. The correction $\delta\Gamma^{CP}$ arises from the CP-odd form factor $h_3^{Z\gamma}$, and is given by

$$\delta\Gamma^{CP}(H \to Z\gamma) = g^2 \frac{(m_H^2 - m_Z^2)^3}{32\pi m_H^3 m_Z^4} |h_3^{Z\gamma}|^2. \quad (19)$$

Using $\mathcal{B}^{\mathrm{SM}}(H \to Z\gamma) = 1.57 \times 10^{-3}$ and $\Gamma_H = 4.1$ MeV [63], Eq. (18) can be expressed in terms of the real and imaginary parts of $h_3^{Z\gamma}$ as

$$\mu^{Z\gamma} = 1 + (1.94\ \mathrm{GeV}^{-2})(\mathrm{Re}[h_3^{Z\gamma}]^2 + \mathrm{Im}[h_3^{Z\gamma}]^2), \quad (20)$$

where the QCD NLO contributions are neglected, as they are expected to be small [20]. Previous limits on $h_3^{Z\gamma}$ have been obtained from e^+e^- colliders [30,31] and γp-induced processes [64]. Using the recent ATLAS measurement of the signal strength, $\mu^{Z\gamma} = 1.3^{+0.6}_{-0.5}$ at $\sqrt{s} = 13.6$ TeV [65], the resulting upper bounds on the CP-violating form factor are presented in Fig. 3, and read

$$|\mathrm{Re}[h_3^{Z\gamma}]|, \qquad |\,\mathrm{Im}[h_3^{Z\gamma}]| \lesssim 0.9\ \mathrm{GeV}(95\%\mathrm{CL}). \quad (21)$$

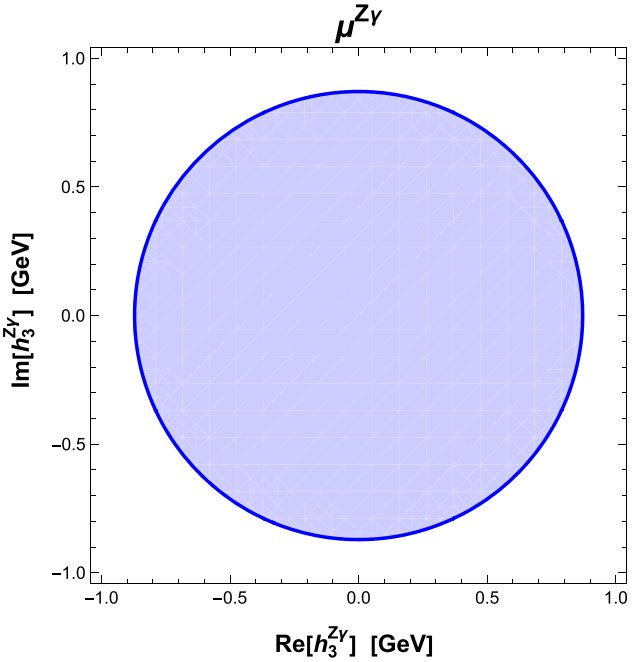


FIG. 3. Allowed region for the real and imaginary parts of the CP-violating form factor $h_3^{Z\gamma}$ at the 95% CL, derived from the signal strength $\mu^{Z\gamma} = 1.3^{+0.6}_{-0.5}$ reported by the ATLAS Collaboration [65].

This value is one order of magnitude tighter than our previous result in Ref. [15], which was based on the combined analysis of the ATLAS and CMS collaborations at $\sqrt{s} = 13$ TeV. Bounds consistent with those shown in Eq. (21) are obtained when using the recent value for $\mu^{Z\gamma}$ reported by the CMS Collaboration [66], where the data collected at center-of-mass energies of 13 and 13.6 TeV are combined. Constraints on CP-violating Higgs couplings can also be derived from electric dipole moments (EDM) [67,68]. In this context, bounds on the $h_3^{Z\gamma}$ form factor were obtained in effective Higgs couplings scenarios [69,70]. Using the notation in Eq. (1), these limits cover the range:

$$10^{-2}\ \mathrm{GeV} \leq |h_3^{Z\gamma}| \leq 10^{-1} - 10^{1}\ \mathrm{GeV}. \quad (22)$$

We emphasize that the upper bounds in Fig. 3, attained from the measured signal strength $\mu^{Z\gamma}$ at the LHC are comparable in size to those derived from EDM observables.

IV. NUMERICAL ANALYSIS

In this section, we present a numerical analysis of the CP-violating effects on the differential partial width in Eq. (12) and on the forward-backward asymmetry. As these observables depend on the real and imaginary parts of the CP-conserving form factor $h_1^{Z\gamma}$, we consider its SM values given in Eq. (2). We focus on charged-leptons final states.

TABLE I. Different scenarios for the real and imaginary parts of the CP-violating form factor $h_3^{Z\gamma}$.

Scenario	$\mathrm{Re}[h_3^{Z\gamma}]$ [GeV]	$\mathrm{Im}[h_3^{Z\gamma}]$ [GeV]
I	0.3	0
II	0	0.3
III	10^{-2}	10^{-1}
IV	10^{-1}	10^{-2}

To analyze the behavior of the differential partial width as a function of $\cos\theta$, we consider four benchmark scenarios for the real and imaginary components of $h_3^{Z\gamma}$. These scenarios are listed in Table I and are chosen to be compatible with the bounds shown in Fig. 3. In scenarios I and II, we separately examine the impact of $\mathrm{Re}[h_3^{Z\gamma}]$ and $\mathrm{Im}[h_3^{Z\gamma}]$, with values close to the upper limits to maximize their contributions. In scenarios III and IV, we consider hierarchical configurations in which one component is dominant at the level of 10^{-1}, while the other is suppressed by one order of magnitude. To make the impact of the CP-odd form factor explicit, we also include the SM case for comparison.

In Fig. 4, we show the differential partial width of the $H \to Z\gamma \to \bar{\ell}\ell\gamma$ decay as a function of $\cos\theta$ for the SM case and the four benchmark scenarios. For scenarios I and II, where larger CP-violating effects are considered, the deviation from the SM prediction is more significant. The contribution from $\mathrm{Re}[h_3^{Z\gamma}]$ modifies the distribution approximately uniformly across the full angular range, whereas $\mathrm{Im}[h_3^{Z\gamma}]$ induces a distortion that is more pronounced for $\cos\theta \leq 0$. In the more realistic scenarios III and IV, the deviations are reduced, although they remain noticeable in the case where the imaginary component dominates. The overall behavior in Fig. 4 is consistent with previous findings reported in Ref. [47].

For the forward-backward asymmetry, we present in Fig. 5 the values of $\mathcal{A}_{FB}$ in the $\mathrm{Re}[h_3^{Z\gamma}]$ vs $\mathrm{Im}[h_3^{Z\gamma}]$ plane. The analysis is restricted to the positive region consistent with the bounds shown in Fig. 3, although a similar behavior is expected throughout the full parameter space. We find that for large values of the imaginary part, the asymmetry can reach $\mathcal{O}(10^{-1})$, an order of magnitude larger than that induced by interference amplitudes [39]. Even for smaller contributions, with $h_3^{Z\gamma} \sim \mathcal{O}(10^{-2})$, the asymmetry can still attain appreciable values of order 10^{-2}. In the SM, the real part of the CP-conserving form factor $h_1^{Z\gamma}$ is of order 10^{-1}, while its imaginary part is about three orders of magnitude smaller. Therefore, the dominant contribution to $\mathcal{A}_{FB}$ in Eq. (17) arises from the interference between $\mathrm{Re}[h_1^{Z\gamma}]$ and $\mathrm{Im}[h_3^{Z\gamma}]$. However, in models with heavy particles, the real and imaginary parts of $h_3^{Z\gamma}$ can reach values close to unity [15,37], without inducing significant deviations from the SM predictions for the $H \to \gamma\gamma$ and $H \to gg$ decays. In such scenarios, the interference between $\mathrm{Im}[h_1^{Z\gamma}]$ and $\mathrm{Re}[h_3^{Z\gamma}]$ may also become relevant. Nevertheless, due to the strong suppression of $\mathrm{Im}[h_1^{Z\gamma}]$ relative to its real part, the magnitude of the asymmetry remains predominantly controlled by $\mathrm{Im}[h_3^{Z\gamma}]$, as shown in Fig. 5. Consequently, cases in which only $\mathrm{Re}[h_3^{Z\gamma}]$ is sizable, such as scenario I in Table I, are less favorable for observing $\mathcal{A}_{FB}$.

It is important to determine whether $\mathcal{A}_{FB}$ can be observed at the LHC or future colliders. To this end, we estimate the expected significance, $Z = S/\sqrt{B}$. We define N_S and N_B as the number of signal and background events

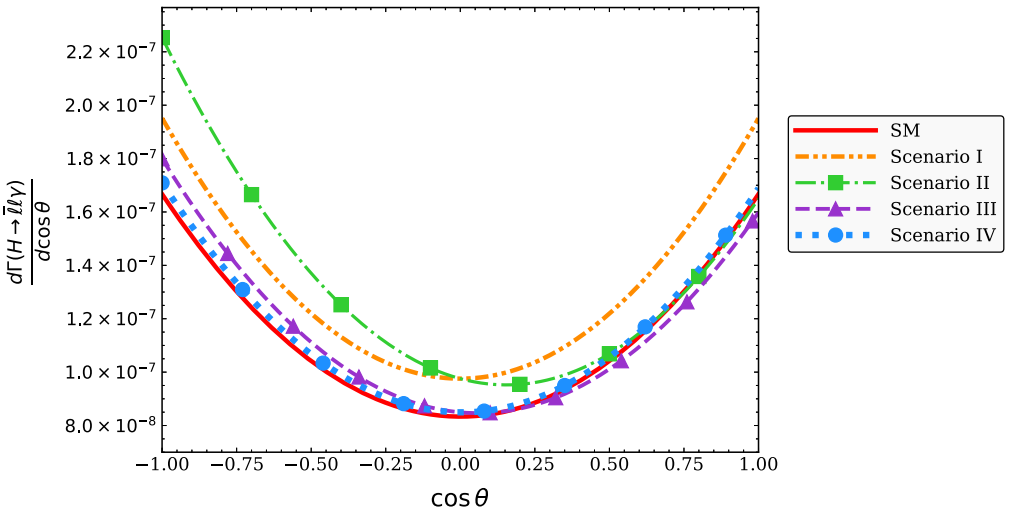


FIG. 4. Differential partial width of the $H \to Z\gamma \to \bar{\ell}\ell\gamma$ decay as a function of $\cos\theta$ for the SM and the benchmark scenarios defined in Table I. The CP-conserving form factor $h_1^{Z\gamma}$ is fixed to its SM electroweak value.

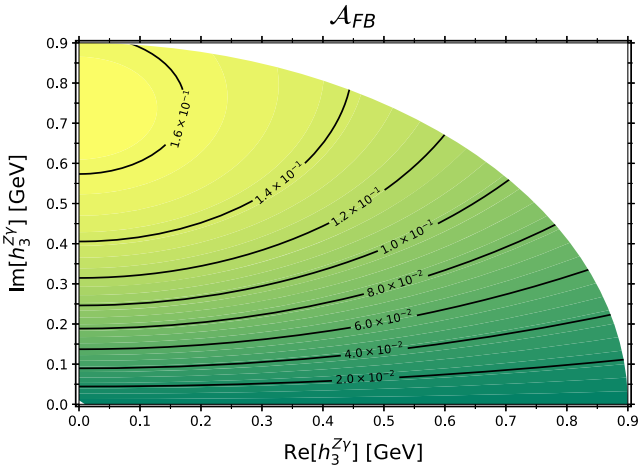


FIG. 5. Forward-backward asymmetry ($\mathcal{A}_{FB}$) in the allowed positive values of the real and imaginary parts of the CP-violating form factor $h_3^{Z\gamma}$.

for the process $gg \to H \to Z\gamma \to \bar{\ell}\ell\gamma$. The asymmetry signal can be interpreted as an excess in N_S, such that $S \sim \mathcal{A}_{FB} N_S$. The background includes both the N_B and the CP-conserving contribution of the $H \to Z\gamma$ decay [39], yielding [26,70]

$$Z = \mathcal{A}_{FB} \frac{N_S}{\sqrt{N_S + N_B}}. \tag{23}$$

The ATLAS Collaboration has recently reported an observed significance of 2.5 standard deviations for the $\bar{\ell}\ell\gamma$ final state [65], combining Run-2 and Run-3 data with 140 fb^{-1} and 165 fb^{-1} luminosities, respectively. Since the irreducible and reducible backgrounds dominate [52,71], we approximate $\sqrt{N_S + N_B} \approx \sqrt{N_B}$. Thus, the relation between the reported ATLAS significance and Eq. (23) is given by $S \sim 2.5\mathcal{A}_{FB}$. Rescaling with luminosity, we obtain

$$Z = \frac{\mathcal{A}_{FB}}{(0.12)} \sqrt{\frac{\mathcal{L}}{3000\ \mathrm{fb}^{-1}}}. \tag{24}$$

This expression agrees with Refs. [39,52], where the signal and backgrounds have been simulated. Equation (24) indicates that for the high-luminosity LHC (HL-LHC) with $\mathcal{L} = 3000$ fb^{-1} and values of $\mathrm{Im}[h_3^{Z\gamma}] \sim \mathcal{O}(10^{-1})$, the $\mathcal{A}_{FB}$ asymmetry could reach the discovery level. The observation of the forward-backward asymmetry would be clear evidence of CP violation.

As pointed out above, the imaginary part of $h_3^{Z\gamma}$ provides the dominant contribution to the forward-backward asymmetry. The values of $\mathrm{Im}[h_3^{Z\gamma}]$ considered so far have been derived solely from experimental constraints. Nevertheless, an absorptive part may arise from loop-induced processes when the particles circulating in the loop can go on-shell. At the one-loop level, this possibility can occur, for instance, in the presence of FCNC couplings of the Higgs and Z bosons. Therefore, the magnitude of $\mathrm{Im}[h_3^{Z\gamma}]$ is model dependent. In Ref. [15], FCNC couplings involving the top quark were found to generate $\mathrm{Re}[h_3^{Z\gamma}]$ of order 10^{-5}. Although an absorptive part can arise for lighter particles, their FCNC contributions are expected to be smaller than those associated with the top quark. Under this assumption, $\mathrm{Im}[h_3^{Z\gamma}]$ would be strongly suppressed, making $\mathcal{A}_{FB}$ challenging to observe at the LHC.

V. CONCLUSIONS

In this work, we analyzed the forward-backward asymmetry in the $H \to Z\gamma \to \bar{f}f\gamma$ decay in the context of recent LHC results. This asymmetry is induced by the presence of a CP-violating form factor and imaginary parts of the $HZ\gamma$ vertex. Although $\mathcal{A}_{FB}$ has been explored in previous studies, we provided its explicit analytical expression for the first time. Furthermore, we studied angular distributions, which are sensitive to CP-violating effects. To estimate the magnitude of the asymmetry, we derived bounds on the real and imaginary components of the CP-violating form factor $h_3^{Z\gamma}$ using current LHC results. We obtained an upper limit of about 0.9 GeV, comparable to those from EDM constraints. We found that the asymmetry can reach values of order 10^{-1} for large $\mathrm{Im}[h_3^{Z\gamma}]$. Under HL-LHC conditions, $\mathcal{A}_{FB}$ could become experimentally accessible at the discovery level. The observation of this forward-backward asymmetry would indicate the existence of new sources of CP violation, which are necessary to explain the matter-antimatter asymmetry.

ACKNOWLEDGMENTS

We thank Arely Cortés-González for valuable discussions and I. García-Márquez for assistance in the preparation of Fig. 6. This work was supported by Sistema Nacional de Investigadoras e Investigadores (SNII). A. I. H.-J. acknowledges additional support from the program "Estancias Posdoctorales por México."

DATA AVAILABILITY

The data supporting the findings of this article consist of numerical results obtained from the calculations described in the manuscript and are available from the corresponding author upon reasonable request.

APPENDIX: KINEMATICS

This appendix presents the kinematics employed in the computation of the $H \to Z\gamma \to \bar{f}f\gamma$ amplitude. We follow the momentum assignments shown in Fig. 6.

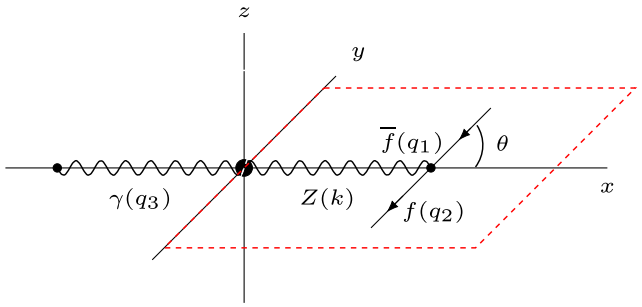


FIG. 6. Kinematic configuration and momentum assignments for the $H \to \bar{f} f \gamma$ decay.

1. Higgs boson rest frame

In the Higgs rest frame, the four-momenta of the Higgs boson, the Z boson, and the photon can be expressed as

$$q^\mu = (m_H, 0), \tag{A1}$$

$$k^\mu = \left(\frac{m_H^2 + m_Z^2}{2m_H}, \vec{k}\right) \tag{A2}$$

$$q_3^\mu = \left(\frac{m_H^2 - m_Z^2}{2m_H}, -\vec{k}\right), \tag{A3}$$

with the magnitude of the three-momentum $\vec{k}$:

$$\|\vec{k}\| = \frac{m_H^2 - m_Z^2}{2m_H}. \tag{A4}$$

2. Z gauge boson rest frame

In the rest frame of the Z boson, the corresponding four-momenta are expressed as

$$k^\mu = (m_Z, 0), \tag{A5}$$

$$q_1^\mu = (m_Z/2, \vec{q}), \tag{A6}$$

$$q_2^\mu = (m_Z/2, -\vec{q}), \tag{A7}$$

where, according to the kinematical configuration shown in Fig. 6, the three-momentum $\vec{q}$ is given by

$$\vec{q} = \frac{\sqrt{m_Z^2 - 4m_\ell^2}}{2}(\cos\theta, \sin\theta, 0). \tag{A8}$$

3. Lorentz invariants

In the evaluation of the squared amplitude for the $H \to Z\gamma \to \overline{\ell}\ell\gamma$ decay, scalar products between four-momenta defined in different reference frames are required. In the Higgs rest frame, the relevant invariants are given by

$$q_1 \cdot q_3 = \frac{(m_H^2 - m_Z^2)}{4}(1 + \cos\theta), \tag{A9}$$

$$q_2 \cdot q_3 = \frac{(m_H^2 - m_Z^2)}{4}(1 - \cos\theta), \tag{A10}$$

which are obtained by performing a Lorentz transformation between frames with velocity $\nu = \frac{m_H^2 - m_Z^2}{m_H^2 + m_Z^2}$.

4. Phase space

The phase space (dR_3) for the $H \to Z\gamma \to \bar{f} f \gamma$ decay can be expressed as

$$dR_3 = \frac{d^3\vec{q}_1}{(2\pi)^3 2E_{\vec{q}_1}} \frac{d^3\vec{q}_2}{(2\pi)^3 2E_{\vec{q}_2}} \times \frac{d^3\vec{q}_3}{(2\pi)^3 2E_{\vec{q}_3}} (2\pi)^4 \delta^4(q - q_1 - q_2 - q_3). \tag{A11}$$

Following the approach in Refs. [72,73], we introduce the identity

$$\int \frac{d^3\vec{k}}{2E_{\vec{k}}} dK \delta^4(k - q_1 - q_2) = 1, \tag{A12}$$

where $K = k^2$ and $E_{\vec{k}} = \sqrt{|\vec{k}|^2 + K}$. The phase space can then be written as

$$dR_3 = \frac{dK}{(2\pi)^5} I_q I_k, \tag{A13}$$

where I_q and I_k are evaluated in the Higgs and Z boson rest frames, respectively, and are given by

$$I_q = \int \frac{d^3\vec{k}}{2E_{\vec{k}}} \frac{d^3\vec{p}_3}{2E_{\vec{p}_3}} \delta^4(q - k - p_3) = \frac{\pi}{2m_H^2}(m_H^2 - m_Z^2), \tag{A14}$$

$$I_k = \int \frac{d^3\vec{q}_1}{2E_{\vec{q}_1}} \frac{d^3\vec{q}_2}{2E_{\vec{q}_2}} \delta^4(k - q_1 - q_2) = \frac{\pi}{4} d\cos\theta. \tag{A15}$$

[1] A. Tumasyan *et al.* (CMS Collaboration), Search for Higgs boson decays to a Z boson and a photon in proton-proton collisions at $\sqrt{s} = 13$ TeV, J. High Energy Phys. 05 (2023) 233.

[2] G. Aad *et al.* (ATLAS Collaboration and CMS Collaboration), Evidence for the Higgs boson decay to a Z boson and a photon at the LHC, Phys. Rev. Lett. **132**, 021803 (2024).

[3] Z.-Q. Chen, L.-B. Chen, C.-F. Qiao, and R. Zhu, Two-loop electroweak corrections to the Higgs boson rare decay process $H \to Z\gamma$, Phys. Rev. D **110**, L051301 (2024).

[4] W.-L. Sang, F. Feng, and Y. Jia, Next-to-leading-order electroweak correction to $H \to Z^0\gamma$, Phys. Rev. D **110**, L051302 (2024).

[5] F.-Z. Chen, Q. Wen, and F. Xu, Higgs decays to $Z\gamma$ and $\gamma\gamma$ in the flavor-gauged two Higgs doublet model, Chin. Phys. C **50**, 063102 (2026).

[6] R. Benbrik, M. Boukidi, M. Ouchemhou, L. Rahili, and O. Tibssirte, Higgs-like particle decays into γZ and $\gamma\gamma$: Fingerprints of some non-supersymmetric models, Nucl. Phys. **B990**, 116154 (2023).

[7] S. Israr and M. Rehman, Higgs decay to $Z\gamma$ in the minimal supersymmetric standard model and its nonholomorphic extension, Eur. Phys. J. Plus **140**, 397 (2025).

[8] E. A. Reyes R., C. A. L. A., O. R. Torrijo G., and D. G. Melo P., Rare Higgs boson decay into a photon and a Z boson in radiatively driven natural supersymmetry, Phys. Rev. D **112**, 095012 (2025).

[9] D. Barducci, L. Di Luzio, M. Nardecchia, and C. Toni, Closing in on new chiral leptons at the LHC, J. High Energy Phys. 12 (2023) 154.

[10] G. Lichtenstein, M. A. Schmidt, G. Valencia, and R. R. Volkas, Z and Higgs boson decays with doubly-charged scalars at one-loop: Current constraints, future sensitivities, and application to lepton-triality models, Nucl. Phys. **B1013**, 116850 (2025).

[11] R. Boto, D. Das, J. C. Romao, I. Saha, and J. P. Silva, New physics interpretations for nonstandard values of $h \to Z\gamma$, Phys. Rev. D **109**, 095002 (2024).

[12] X.-G. He, Z.-L. Huang, M.-W. Li, and C.-W. Liu, The SM expected branching ratio for $h \to \gamma\gamma$ and an excess for $h \to Z\gamma$, J. High Energy Phys. 10 (2024) 135.

[13] K. Cheung and C. J. Ouseph, Interpretation of excess in $H \to Z\gamma$ using a light axion-like particle, Phys. Rev. D **110**, 055016 (2024).

[14] A. Kachanovich, J. Kimus, S. Lowette, and M. H. G. Tytgat, On new physics off the Z peak in $H \to \ell^+\ell^-\gamma$, J. High Energy Phys. 06 (2025) 043.

[15] A. I. Hernández-Juárez, R. Gaitán, and R. Martinez, $H \to Z\gamma$ decay and CP violation, Phys. Rev. D **111**, 015001 (2025).

[16] R. N. Cahn, M. S. Chanowitz, and N. Fleishon, Higgs particle production by $Z \to H\gamma$, Phys. Lett. B **82**, 113 (1979).

[17] L. Bergstrom and G. Hulth, Induced Higgs couplings to neutral bosons in e^+e^- collisions, Nucl. Phys. **B259**, 137 (1985); **B276**, 744(E) (1986).

[18] J. F. Gunion, H. E. Haber, G. L. Kane, and S. Dawson, *The Higgs Hunter's Guide*, Vol. 80 (Westview Press, Boulder, Colorado, 2000).

[19] R. Decker, M. Nowakowski, and D. Woitschitzky, The $Z^0 \to H\gamma$ decay in two-Higgs-doublet models, Phys. Lett. B **255**, 605 (1991).

[20] M. Spira, A. Djouadi, and P. Zerwas, QCD corrections to the $HZ\gamma$ coupling, Phys. Lett. B **276**, 350 (1992).

[21] R. Bonciani, V. Del Duca, H. Frellesvig, J. M. Henn, F. Moriello, and V. A. Smirnov, Next-to-leading order QCD corrections to the decay width $H \to Z\gamma$, J. High Energy Phys. 08 (2015) 108.

[22] T. Gehrmann, S. Guns, and D. Kara, The rare decay $H \to Z\gamma$ in perturbative QCD, J. High Energy Phys. 09 (2015) 038.

[23] A. I. Hernández-Juárez, A. Moyotl, and G. Tavares-Velasco, New estimate of the chromomagnetic dipole moment of quarks in the standard model, Eur. Phys. J. Plus **136**, 262 (2021).

[24] G. J. Gounaris, J. Layssac, and F. M. Renard, New and standard physics contributions to anomalous Z and γ self-couplings, Phys. Rev. D **62**, 073013 (2000).

[25] A. I. Hernández-Juárez, G. Tavares-Velasco, and A. Fernández-Téllez, New evaluation of the HZZ coupling: Direct bounds on anomalous contributions and CP-violating effects via a new asymmetry, Phys. Rev. D **107**, 115031 (2023).

[26] R. M. Godbole, D. J. Miller, and M. M. Muhlleitner, Aspects of CP violation in the HZZ coupling at the LHC, J. High Energy Phys. 12 (2007) 031.

[27] A. I. Hernández-Juárez, A. Moyotl, and G. Tavares-Velasco, Bounds on the absorptive parts of the chromomagnetic and chromoelectric dipole moments of the top quark from LHC data, Eur. Phys. J. Plus **137**, 925 (2022).

[28] A. I. Hernández-Juárez and R. Gaitán, CP violation in the HZZ vertex and left-right asymmetries, Phys. Rev. D **112**, 033006 (2025).

[29] S. Taheri Monfared, S. Fayazbakhsh, and M. Mohammadi Najafabadi, Exploring anomalous $HZ\gamma$ couplings in γ-proton collisions at the LHC, Phys. Lett. B **762**, 301 (2016).

[30] K. Hagiwara, S. Ishihara, J. Kamoshita, and B. A. Kniehl, Prospects of measuring general Higgs couplings at e^+e^- linear colliders, Eur. Phys. J. C **14**, 457 (2000).

[31] S. D. Rindani and P. Sharma, Angular distributions as a probe of anomalous ZZH and γZH interactions at a linear collider with polarized beams, Phys. Rev. D **79**, 075007 (2009).

[32] A. Y. Korchin and V. A. Kovalchuk, Polarization effects in the Higgs boson decay to γZ and test of CP and CPT symmetries, Phys. Rev. D **88**, 036009 (2013).

[33] I. Ahmed, U. Hasan, S. Iqbal, M. Junaid, B. Tariq, and A. Uzair, Analysis of final state lepton polarization-dependent observables in $H \to \ell^+\ell^-\gamma$ in the SM at loop level, J. High Energy Phys. 05 (2024) 187.

[34] U. Hasan, A. Uzair, M. Junaid, B. Tariq, I. Ahmed, and S. Iqbal, Polarization-dependent observables in $H \to \ell^+\ell^-\gamma$ in the SM, Prog. Theor. Exp. Phys. **2025**, 033B11 (2025).

[35] V. Hankele, G. Klamke, D. Zeppenfeld, and T. Figy, Anomalous Higgs boson couplings in vector boson fusion at the CERN LHC, Phys. Rev. D **74**, 095001 (2006).

[36] A. Y. Korchin and V. A. Kovalchuk, Higgs Boson Decay to γZ and Test of CP and CPT Symmetries, Acta Phys. Pol. B **44**, 2121 (2013).

[37] S.-P. He, Higgs boson to γZ decay as a probe of flavor-changing neutral Yukawa couplings, Phys. Rev. D **102**, 075035 (2020).

[38] D. Binosi and L. Theußl, JaxoDraw: A Graphical user interface for drawing Feynman diagrams, Comput. Phys. Commun. **161**, 76 (2004).

[39] Y. Chen, A. Falkowski, I. Low, and R. Vega-Morales, New observables for CP violation in Higgs decays, Phys. Rev. D **90**, 113006 (2014).

[40] G. Eilam, J. L. Hewett, and A. Soni, CP asymmetries induced by particle widths: Application to top quark decays, Phys. Rev. Lett. **67**, 1979 (1991).

[41] D. Atwood, G. Eilam, M. Gronau, and A. Soni, Enhancement of CP violation in $B^{\pm} \to K_i^{\pm} D^0$ by resonant effects, Phys. Lett. B **341**, 372 (1995).

[42] I. Bediaga, I. I. Bigi, A. Gomes, G. Guerrer, J. Miranda, and A. C. d. Reis, On a CP anisotropy measurement in the Dalitz plot, Phys. Rev. D **80**, 096006 (2009).

[43] M. Nowakowski and A. Pilaftsis, CP-odd phenomena due to finite width effects of the top quark, Mod. Phys. Lett. A **06**, 1933 (1991).

[44] J. Berger, M. Blanke, and Y. Grossman, A new CP violating observable for the LHC, J. High Energy Phys. 08 (2011) 033.

[45] Y. Gao, A. V. Gritsan, Z. Guo, K. Melnikov, M. Schulze, and N. V. Tran, Spin determination of single-produced resonances at hadron colliders, Phys. Rev. D **81**, 075022 (2010).

[46] S. Bolognesi, Y. Gao, A. V. Gritsan, K. Melnikov, M. Schulze, N. V. Tran, and A. Whitbeck, Spin and parity of a single-produced resonance at the LHC, Phys. Rev. D **86**, 095031 (2012).

[47] I. Anderson *et al.*, Constraining anomalous HVV interactions at proton and lepton colliders, Phys. Rev. D **89**, 035007 (2014).

[48] A. Kachanovich, U. Nierste, and I. Nišandžić, Higgs boson decay into a lepton pair and a photon revisited, Phys. Rev. D **101**, 073003 (2020).

[49] H.-R. He, X. Wan, and Y.-K. Wang, Anomalous $H \to ZZ \to 4\ell$ decay and its interference effects on gluon–gluon contribution at the LHC, Chin. Phys. C **44**, 123101 (2020).

[50] K.-Y. Feng, X. Wan, Y.-K. Wang, and C. Wu, Exploring HVV amplitudes with CP violation using decomposition and the on-shell scattering amplitude method*, Chin. Phys. C **47**, 033106 (2023).

[51] A. Y. Korchin and V. A. Kovalchuk, Angular distribution and forward–backward asymmetry of the Higgs-boson decay to photon and lepton pair, Eur. Phys. J. C **74**, 3141 (2014).

[52] X. Chen, G. Li, and X. Wan, Probe CP violation in $H \to \gamma Z$ through forward-backward asymmetry, Phys. Rev. D **96**, 055023 (2017); **103**, 099902(A) (2021).

[53] A. V. Gritsan *et al.*, Snowmass White Paper: Prospects of CP-violation measurements with the Higgs boson at future experiments, arXiv:2205.07715.

[54] A. I. Hernández-Juárez, A. Moyotl, and G. Tavares-Velasco, Contributions to ZZV^* $(V = \gamma, Z, Z')$ couplings from CP violating flavor changing couplings, Eur. Phys. J. C **81**, 304 (2021).

[55] A. I. Hernández-Juárez, R. Gaitán, and G. Tavares-Velasco, FCNC contributions to the $Z\gamma V^*$ vertex, polarizations and bounds on $Z\bar{t}q$ couplings, Int. J. Mod. Phys. A **40**, 2550132 (2025).

[56] A. I. Hernández-Juárez, G. Tavares-Velasco, and A. Moyotl, Chromomagnetic and chromoelectric dipole moments of quarks in the reduced 331 model, Chin. Phys. C **45**, 113101 (2021).

[57] J. I. Aranda, D. Espinosa-Gómez, J. Montaño, B. Quezadas-Vivian, F. Ramírez-Zavaleta, and E. S. Tututi, Flavor violation in chromo- and electromagnetic dipole moments induced by Z′ gauge bosons and a brief revisit of the Standard Model, Phys. Rev. D **98**, 116003 (2018).

[58] J. I. Aranda, T. Cisneros-Pérez, J. Montaño, B. Quezadas-Vivian, F. Ramírez-Zavaleta, and E. S. Tututi, Revisiting the top quark chromomagnetic dipole moment in the SM, Eur. Phys. J. Plus **136**, 164 (2021).

[59] R. Mertig, M. Bohm, and A. Denner, FEYN CALC: Computer algebraic calculation of Feynman amplitudes, Comput. Phys. Commun. **64**, 345 (1991).

[60] V. Shtabovenko, R. Mertig, and F. Orellana, New Developments in FeynCalc 9.0, Comput. Phys. Commun. **207**, 432 (2016).

[61] V. Shtabovenko, R. Mertig, and F. Orellana, FeynCalc 9.3: New features and improvements, Comput. Phys. Commun. **256**, 107478 (2020).

[62] V. Shtabovenko, R. Mertig, and F. Orellana, FeynCalc 10: Do multiloop integrals dream of computer codes?, Comput. Phys. Commun. **306**, 109357 (2025).

[63] D. de Florian *et al.* (LHC Higgs Cross Section Working Group), Handbook of LHC Higgs cross sections: 4. Deciphering the nature of the Higgs sector, CERN Yellow Rep. Monogr. **2**, 1 (2017).

[64] A. Senol, A. T. Tasci, I. T. Cakir, and O. Cakir, Anomalous, $HZ\gamma$ couplings in photon-induced collisions at the LHC, Mod. Phys. Lett. A **29**, 1450186 (2014).

[65] G. Aad *et al.* (ATLAS Collaboration), Search for the Higgs boson decay to a Z boson and a photon in pp collisions at $\sqrt{s} = 13$ TeV and 13.6 TeV with the ATLAS detector, Phys. Lett. B **876**, 140313 (2026).

[66] CMS Collaboration, Search for the rare Higgs boson decay H to Z gamma in proton-proton collisions at $\sqrt{s} = 13$ TeV and 13.6 TeV, Technical Report No. CMS-PAS-HIG-25-010, CERN, Geneva, 2026.

[67] Y. T. Chien, V. Cirigliano, W. Dekens, J. de Vries, and E. Mereghetti, Direct and indirect constraints on CP-violating Higgs-quark and Higgs-gluon interactions, J. High Energy Phys. 02 (2016) 011.

[68] S. Weinberg, Larger Higgs-boson-exchange terms in the neutron electric dipole moment, Phys. Rev. Lett. **63**, 2333 (1989).

[69] S. Dwivedi, D. K. Ghosh, B. Mukhopadhyaya, and A. Shivaji, Constraints on CP-violating gauge-Higgs operators, Phys. Rev. D **92**, 095015 (2015).

[70] S. Dwivedi, D. K. Ghosh, B. Mukhopadhyaya, and A. Shivaji, Distinguishing CP-odd couplings of the Higgs boson to weak boson pairs, Phys. Rev. D **93**, 115039 (2016).

[71] J. S. Gainer, W.-Y. Keung, I. Low, and P. Schwaller, Looking for a light Higgs boson in the $Z\gamma \to \ell\bar{\ell}\gamma$ channel, Phys. Rev. D **86**, 033010 (2012).

[72] H.-Y. Cheng, C.-Y. Cheung, W. Dimm, G.-L. Lin, Y. C. Lin, T.-M. Yan, and H.-L. Yu, Heavy quark and chiral symmetry predictions for semileptonic decays $\bar{B} \to \mathrm{D}(D^*)\pi\ell\bar{\nu}$, Phys. Rev. D **48**, 3204 (1993).

[73] N. Cabibbo and A. Maksymowicz, Angular correlations in K_{e4} decays and determination of low-energy $\pi - \pi$ phase shifts, Phys. Rev. **137**, B438 (1965); Phys. Rev. **168**, 1926(E) (1968).